Received: 21 October 2024 | Revised: 11 December 2024 | Accepted: 24 January 2025 | Published online: 14 February 2025

Journal of Optics and Photonics Research
2026, Vol. 3(1) 19–29
DOI: 10.47852/bonviewJOPR52024594

BON VIEW PUBLISHING

RESEARCH ARTICLE

Optics of Jumping Sundogs

Alberto Tufaile[1,*] and Adriana Pedrosa Biscaia Tufaile[1]

[1]*School of Arts, Sciences and Humanities, University of São Paulo, Brazil*

Abstract: Jumping sundogs, or crown flashes, are a rare and interesting atmospheric phenomenon characterized by beams of light dancing across the sky. Despite their rarity, social media videos have captured numerous instances of this phenomenon under seemingly similar conditions. By analyzing these videos, we have investigated the structure and dynamics of jumping sundogs. Our analysis reveals that these events require specific ice crystal types and atmospheric conditions. The distinctive feather-like luminescence of jumping sundogs is attributed to the orientation of ice crystals influenced by electric fields within the cloud. These crystals interact with sunlight, creating the observed luminous pattern. We propose that electrical charges near the base of the crown flash generate an electric field that guides the ice crystal orientation. Jumping sundogs might exhibit a "memory effect", because in a certain temperature range, their orientation could depend on their past state (aligned), unlike the random orientation at higher temperatures. Jumping sundogs are a type of critical phenomena, where ice crystals align in a specific direction below a critical temperature and orient randomly above it.

Keywords: crown flash, jumping sundogs, dynamical systems, ferrofluids, Ising model

1. Introduction

The wonders of nature inspire us to explore the fundamental workings of the world around us. For example, a jumping sundog, also known as "crown flash", is a rare, dazzling flash of light appears above the clouds [1], as it is shown in Figure 1. Experts in atmospheric optics believe electric fields within clouds shift ice crystals' orientation, reflecting sunlight and creating beams of light that dance across the sky [1]. Based on these assumptions, the phenomenon requires the presence of specific ice crystals in the atmosphere, as well as well-determined thermodynamic conditions [2]. Despite its rarity, several social media videos capture this phenomenon under seemingly similar atmospheric circumstances, with the person recording the crown flash commonly reacting with breathtaking surprise. These videos were recorded in different parts of the world, and sometimes we have the same phenomenon recorded by two different persons, showing the importance of the observer's position. We consider these records to be extremely important for understanding these events. By analyzing social media videos, we have investigated the structure and dynamics of jumping sundogs.

Let's exemplify some of the characteristics of crown flashes that we observed in some of these videos. First, many of these leaping sundogs exhibit a distinctive, feather-like luminescence. The feather-like structure characterizes the jumping sundog in the observed videos, often appearing as if it were supported by a cloud. These leaping sundogs, characterized by a curved plume with intense light at its core that narrows at the base and widens outwards, typically appear within the region associated with the 22-degree halo. Our analysis of various videos suggests that electrical charges within the cloud, near the base of the crown flash, generate an electric field. This field then guides the orientation of ice crystals, which subsequently interact with sunlight to create the observed luminous pattern. Another intriguing aspect of this phenomenon is the plume's movement. Initially anchored to the cloud at its base, it exhibits oscillations around this point before transitioning to whip-like motions, with a frequency of these oscillations of around two to three hertz. The duration of the recorded phenomena can last up to 2 min.

Due to limited research, much remains unknown about this phenomenon, and this study aims to understand the complex physics behind jumping sundogs. By combining knowledge from various physics fields, we can develop a comprehensive theory. This research bridges different scientific disciplines. We will discuss ice crystal dynamics, experimental systems, and potential statistical mechanics models to explore phase transitions within this system. Finally, we will summarize our key findings.

2. Literature Review

Our research combines physics and atmospheric science to study ice crystals, such as snowflake formation [2] and liquid crystals [3–5]. In this article, we employ the Ising model to understand the formation of ice crystals in clouds and the phenomenon of jumping sundogs. The Ising model [6, 7], originally designed to study magnetism, has proven remarkably versatile for the system that we are studying here. It has been applied to diverse fields, including information technology [8], finance [9], and chemistry [10]. This model's strength lies in its ability to capture the essence of complex systems by simplifying them to their core interactions. By doing so, it allows researchers to identify hidden patterns and predict emergent behavior.

By analyzing atmospheric optical phenomena like jumping sundogs and crown flashes, we can develop innovative remote

***Corresponding author:** Alberto Tufaile, School of Arts, Sciences and Humanities, University of São Paulo, Brazil. Email: tufaile@usp.br

Figure 1

(a) Two images of jumping sundogs observed in different places around the world, showing their position in relation to the sun. (b) Formation of crown flashes is illustrated in the diagram, with electrical charges within the cloud generating an electric field and guiding the motion of microscopic ice crystals interacting with sunlight. Typically, the observed light pattern is perpendicular to the orientation of the ice crystals. (c) Jumping sundog with the appearance of a feather next to a sundog that shows color separation. (d) The jumping sundog of the previous image moves to a region away from the sundog

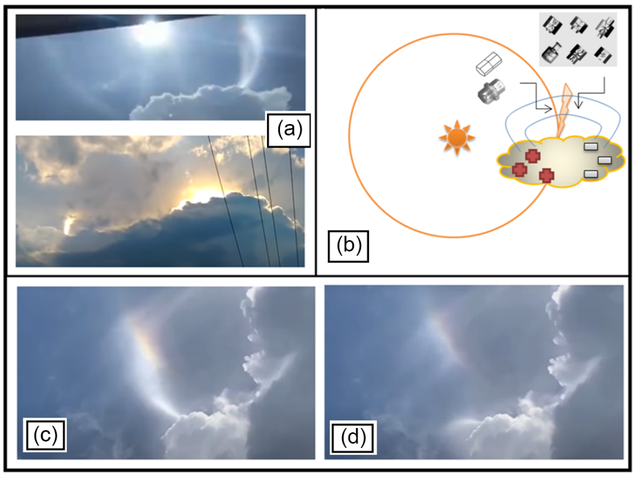

Figure 2

We showcase a plot illustrating the impact of ferrofluid dilution. Our study investigates how the density of the ferrofluid influences the magneto-optical pattern, particularly when the ferrofluid is diluted. Without dilution, the formation of a light pattern is not observable. However, as we augment the concentration of mineral oil, effectively diluting the original ferrofluid, a more distinct and well-defined luminous pattern in the magneto-optical display emerges. In this graph, *n* is the additional volume of mineral oil added to dissolve the amount of original ferrofluid, if we consider the initial volume of ferrofluid as 1

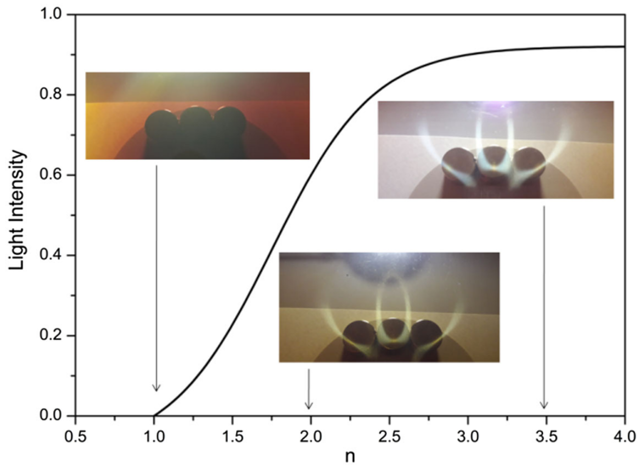

sensing techniques [11]. These techniques can reveal valuable information about the properties of ice crystals within clouds, such as their size, shape, and orientation. Cloud dynamics explores the physical processes driving cloud formation and evolution, while remote sensing employs various techniques to collect data about clouds without direct physical interaction. Both fields contribute to our understanding of how clouds interact with light, a key factor in Earth's energy balance [12, 13]. By analyzing how clouds scatter light, we can infer properties like ice crystal shape and size [14–16]. Sophisticated algorithms using Ising model, such as genetic algorithms, help extract valuable information from remote sensing data [17]. For the specific case of jumping sundogs, in the literature, the atmospheric electrical fluctuations can re-align ice crystals within a cumulonimbus cloud, causing sunlight to reflect or refract above the cloud, resulting in phenomena similar to the crown flash [18].

3. Research Methodology

3.1. Material and methods

Our inspiration comes from social media videos showing jumping sundogs sparked the research (see a list of videos in the supplementary material), and our modeling approach is based on dynamical systems used to understand the movement of ice crystals. Our experimental system used is based on ferrofluids (magnetic fluids) to mimic the optical effects of jumping sundogs. The ferrofluid is a mixture of tiny magnetic particles suspended in oil and can interact with light when a magnetic field nudges them around. These stable suspensions, typically formulated with 5% magnetic solids, 10% stabilizer, and 85% oil, contain magnetic nanoparticles about 10 nanometers in diameter. The ferrofluid used (EFH1) has a specific saturation magnetization and magnetic volume fraction, but you can find those details from the manufacturer (Ferrotec).

In Figure 2, we present a plot showing the effect of the dilution of the ferrofluid. We studied how the density of the ferrofluid affects the magneto-optical pattern, that is, when we dilute the ferrofluid what happens with the light pattern. If we do not dilute the ferrofluid, we will not observe the formation of a light pattern. As we increase the concentration of mineral oil, that is, diluting the original ferrofluid, we have a greater definition of the formation of the luminous pattern of the magneto-optical pattern [19]. In this way, we see that there is a range of ferrofluid concentration values most suitable for the formation of light patterns. In Figure 3, we present the diagram of our experimental apparatus.

Figure 3

Diagram of the experimental setup, showing the observer, the ferrofluid-filled Ferrocell (simulating the cloud), and the light source (simulating the sun)

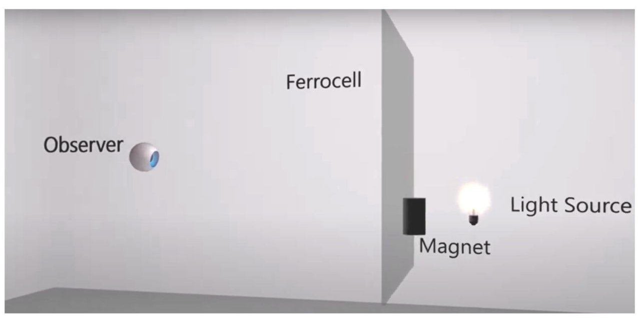

Figure 4
Image of the distribution of spins 1 (black) and −1 (white) using the Ising model at the critical temperature in (a) representing the cloud. Plot of the mean spin and mean energy in (b) from our Ising model for the crystal orientation system

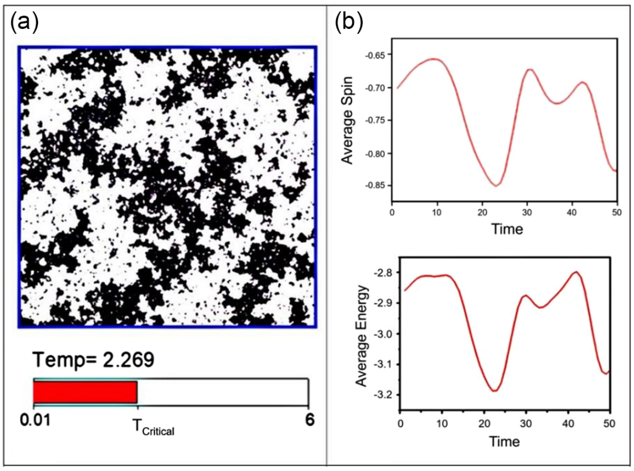

We have used condensed matter models, in order to explore the possible potential phase transitions (sudden changes) in the ice crystals, such as the Ising model. The Hamiltonian of the Ising model is a mathematical expression that encapsulates the energy interactions within a system of magnetic spins. In this model, each lattice site is associated with a discrete spin variable, typically taking values of $+1$ or -1, representing the orientation of a magnetic moment. The Hamiltonian is composed of two main components: the interaction between neighboring spins and the influence of an external magnetic field. The interaction term, often represented by the symbol J, quantifies the preference for neighboring spins to align ($J > 0$) or anti-align ($J < 0$). Meanwhile, the external magnetic field is denoted by the symbol h. The Ising model Hamiltonian, denoted as H, is expressed as the sum of the product of spin pairs and the product of the external field and individual spins.

Mathematically, it can be written as:

$$H = -J \sum \left(\sigma_i \sigma_j\right) - h \sum \sigma_i \tag{1}$$

where the first sum is over pairs of adjacent spins (every pair is counted once), the sums are taken over all pairs of neighboring spins and all individual spins, respectively.

Figure 5
In this figure, we have a diagram illustrating, (a) the process of ice crystal formation and expansion within the cloud. Alongside the crystal's growth, there is also precipitation, and as it descends, it reflects light and (b) there is a three-dimensional image depicting a typical ice crystal in the phase diagram for ice crystal formation

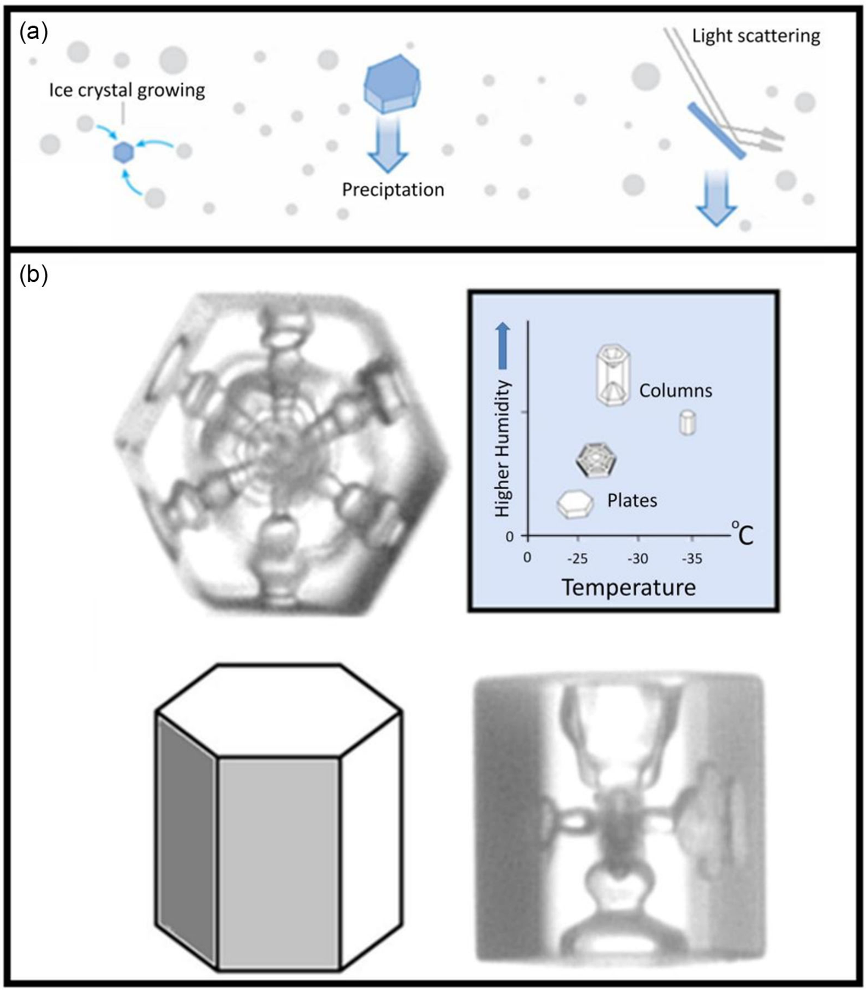

We have used Monte Carlo simulation techniques to update the spins iteratively based on the Metropolis algorithm. This involves calculating the change in energy due to a proposed spin flip and accepting or rejecting the flip based on a probability criterion. This approach enabled us to study thermodynamic observables such as magnetization, susceptibility, and specific heat to analyze the behavior of the system. This adaptation allows us to model a system with fixed compass needles on a lattice of (512 × 512), and we can explore the collective behavior of the system as a function of temperature and interaction parameters which is shown in Figure 4.

We are proposing a mechanism with three parts: electric fields and ice crystal alignment, temperature-dependent phases, and electric field disruption. For the case of electric fields and ice crystal alignment, we have a similar case of compass needles, ice crystals might align with an electric field within a cloud (like a compass and Earth's magnetic field). The temperature-dependent phases occur when the crystals might have a critical temperature below which they align and above which they become random [20, 21]. The electric field disruption is represented by cloud charges that could disrupt this alignment through their electric field, influencing the crystals' behavior and causing the "jumps".

3.2. Motion of charged ice crystals in clouds

Ice crystal formation in clouds is a complex process influenced by various factors [22]. The triangular shape of water molecules and the angle of hydrogen bonds lead to the hexagonal structure of ice crystals. Slow freezing, specific temperature and humidity conditions, airflow, and electrical fields all play significant roles in shaping ice crystal structures. By understanding these factors, we can gain insights into the intricate process of ice crystal formation in clouds.

Figure 5(a) illustrates ice crystal formation and growth within a cloud. As crystals grow and descend, they reflect light. This process occurs within a suspension of air, liquid water droplets, and water vapor. Figure 5(b) presents a 3D image of a typical ice crystal formed between −25 °C and −35 °C. Hexagonal columns form under specific humidity conditions. The ice crystal morphology diagram, plotting temperature against ice supersaturation, helps us understand the factors influencing ice crystal shapes. Interestingly, these crystals can even contain air bubbles.

Clouds are complex systems where ice crystals form and grow (Figure 6). Ice nuclei catalyze the formation of frozen droplets, which then grow by consuming surrounding liquid droplets. This process leads to various ice crystal shapes. Sundogs are optical phenomena resulting from the interaction of sunlight with these complex cloud ice crystals [18, 23]. The presence of ice crystals in the atmosphere, along with other atmospheric factors like impurities and gas composition, influences crystal growth and shape. This diversity in crystal structure can impact their interaction with light, leading to phenomena like "jumping sundogs".

According to experiments performed by Vonnegut [24] and Graves et al. [25], when ice crystals form in a supercooled cloud, they can reflect light like tiny mirrors. This phenomenon is similar to sun pillars observed in the atmosphere. By introducing an electric field, we can manipulate the orientation of these ice crystals. The electric field induces electrical dipoles in the crystals, causing them to reorient and move. Wirowski [18] developed an equation describing the rotational motion of individual crystals, considering factors like charge distribution, large-angle rotation, external forces, and air resistance (μ, α, β_1, and γ). This equation can be used to model the collective behavior of electrically charged ice crystals in a cloud, representing their nonlinear vibrations in a continuous, two-dimensional form:

Figure 6

A comparison is presented between dipoles in the electric field and the magnetic field. (a) We observe ice crystals forming the sundog, while (b) ferrofluid microneedles are displaced and oriented by the magnetic field. Below, we observe the jumping laserdog, whose formation relies on the orientation of the microneedles in the ferrofluid. In this scenario, it's noticeable that light disperses perpendicularly to the orientation of the microneedles, which align with the magnetic field. (c) Light interacts with ice crystals. (d) Diagram of a rigid rotor (ice crystal column) with periodic impulses

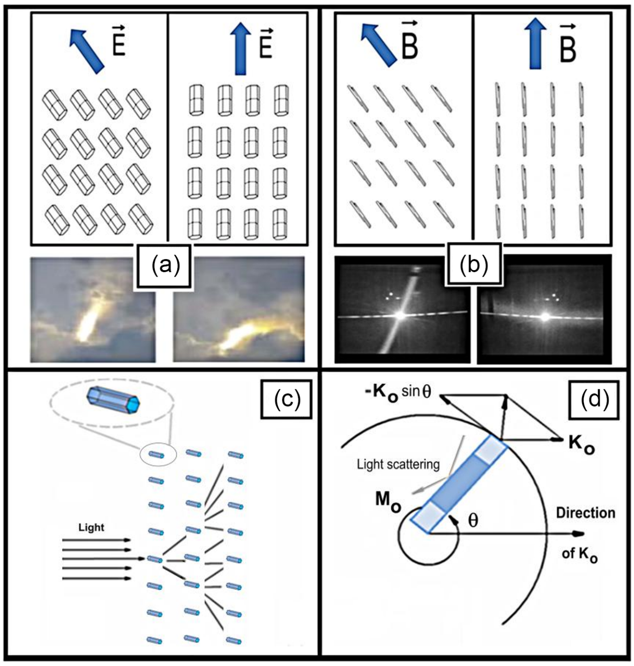

$$\frac{\partial^2\theta(x,y,t)}{\partial t^2} + \Psi^2 \frac{\partial\theta(x,y,t)}{\partial t} + \alpha^2\left(\frac{\partial^2\theta(x,y,t)}{\partial x^2} + \Psi^2 \frac{\partial^2\theta(x,y,t)}{\partial y^2}\right) + - \beta_1{}^2\theta(x,y,t)\gamma(\theta(x,y,t))^3 = -M^E(x,y,t) \quad (2)$$

where M^E is the external forcing vibrations moment. Equation (2) provides a continuous, two-dimensional description of the nonlinear vibrational behavior of a cloud of electrically charged ice crystals. This model accounts for the continuous distribution of electric charge on the crystal surfaces, the possibility of large-angle rotations, the influence of external forcing, and the effects of air resistance.

The torque exerted τ on each ice crystal with dipole moment $\boldsymbol{p}$ by the field $\boldsymbol{E}$ can be mathematically expressed as follows:

$$\tau = E \times p \quad (3)$$

This example equation highlights the fundamental relationship between the electric field, the crystal's own properties (dipole moment), and the resulting torque that influences its orientation, and we use a dynamical system known as a two-dimensional circle map, as illustrated in Figure 6(d), as described by Tufaile et al. [22], to express the motion of ice crystals hexagonal columns:

$$\theta_{n+1} = \theta_n + \Omega - \frac{K}{2\pi}\sin(2\pi\theta_n) + br_n(mod\ 1) \quad (4)$$

$$r_{n+1} = br_n - \frac{K}{2\pi}\sin(2\pi\theta_n) \quad (5)$$

Here, θ_n represents the angle of the rotor after the n-th impulse due to the electric field, r_n is proportionate to the angular velocity, Ω denotes the frequency ratio between the electric field and ice crystal oscillation, b is the damping constant associated with the contraction of the phase space, and K stands for the coupling strength.

The oscillations of the jumping sundog were measured from video of the plume-like motion of Figure 7(a), and they were represented in the plot of Figure 7(b). A simulation is shown in Figure 7(c), with $K = 6.01$, $\Omega = 0.6$, and $b = 0.2$. The reconstructed attractor for this time series, resembling a "rhino horn", is displayed in Figure 7(d).

4. Magneto-Optics of Ferrofluids

Now that we have a mechanical model that shows the movement of a hexagonal rod, let's explore the collective behavior of several crystals interacting with each other. To begin with, let's understand how images are formed in a ferrofluid subjected to a magnetic field. We can compare images between jumping sundogs and patterns observed in magneto-optics of ferrofluids in Figure 8. Considering that in both cases we have a light source interacting with particles in suspension, we see that the light pattern forms a plume with the base close to the place where the charges are concentrated.

We explored this type of light pattern formation in our previous work on luminous horocycles [19, 23], for the case of horocycles of Figure 9. The formation of the pattern by a point light source can be understood as a scattering of light perpendicular to the orientation of the field, as the particles align with the field. The different patterns observed in the jumping sundogs can be modeled here for different "charges" configurations shown in Figure 9(b)–(c).

At this point, we will make a simplified model of the formation and orientation of microneedles in ferrofluids with a model based on compass-type magnetic dipoles in a square arrangement. In order to do this, we will use Figure 10.

Taking into account both the light source and the magnetic field, the light pattern consistently aligns perpendicularly to the external field in Figure 10(a). This correlation stems from the alignment of particles resembling small needles with the applied magnetic field of Figure 10(b). This observation prompts us to contemplate a model involving compass needles arranged in a square lattice of Figure 10(c) in the presence of a magnet. In Figure 10(d), we

Figure 7

(a) We depict two images of an oscillating jumping sundog. (b) A graph illustrating the oscillation of the jumping sundog plume, corresponding to the variation in the angle of the ice crystals, as depicted in the inset. (c) The time series obtained using our model of rigid rotor with impulse. The plot of the attractor of this time series is shown in (d)

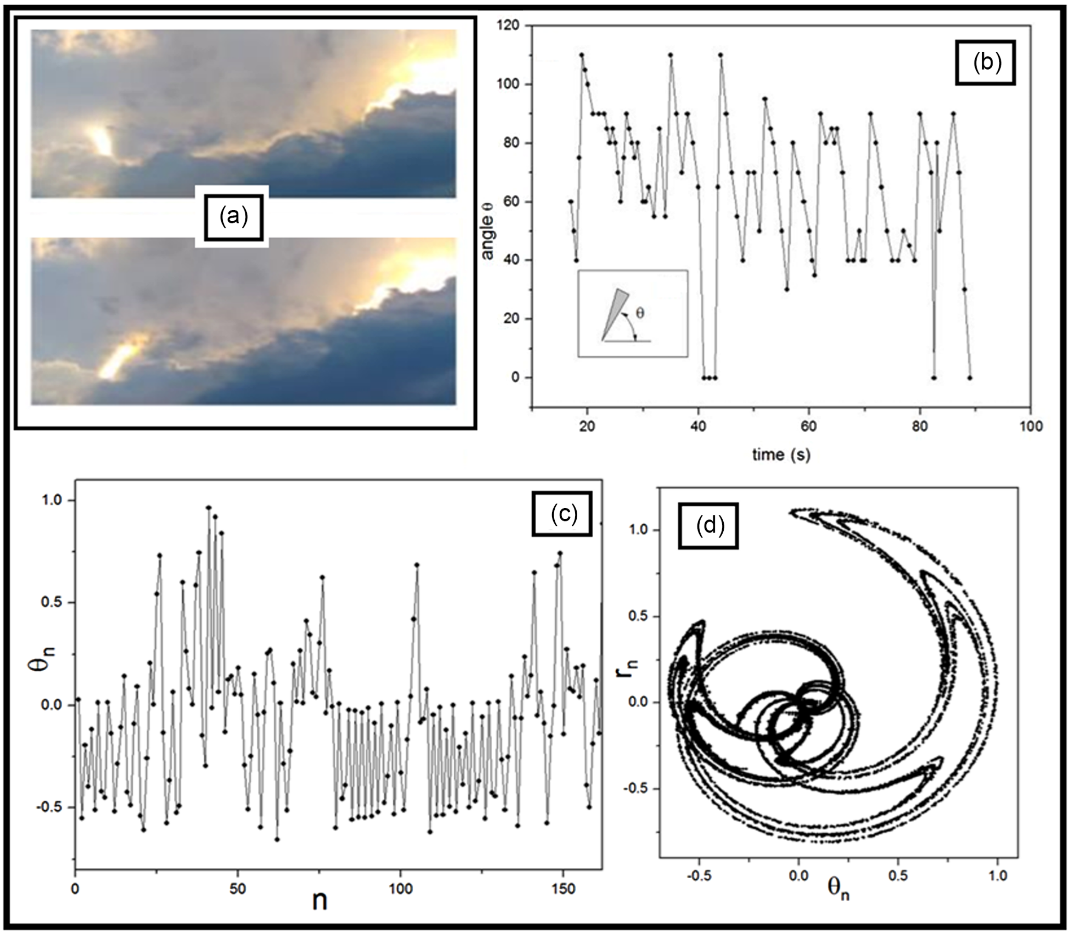

Figure 8

(a) A jumping sundog is depicted, giving rise to a plume adjacent to it. (b) A magnet generates a magnetic field in a thin film of ferrofluid, resulting in an optical pattern resembling a feather. Notably, the light intensity is most pronounced at the plume's base near the "magnetic charge", and in this region, the plume appears narrower, like the jumping sundog pattern. The light source, which is to the right of the image in both cases (the sun in (a) and a lamp in (b)), is not shown

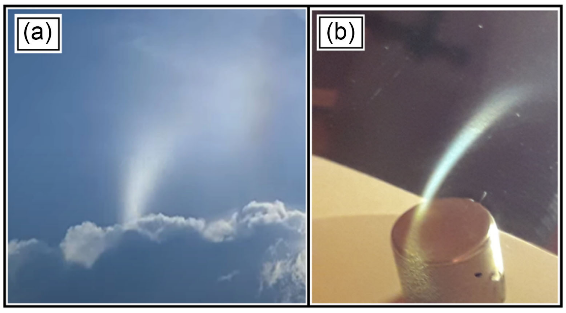

Figure 9

A dipolar field and a light horocycle in (a), where the bright spot at the top in the horocycle represents the light source. Within this field, structures resembling isoclines form, with lines running perpendicular to the magnetic field. The green light pattern, perpendicular to the field lines, is reminiscent of a horocycle. The bottom row displays a sequence of images using different magnetic field sources. Image (b) depicts the horocycle for a monopolar configuration, (c) shows the light pattern for a dipolar configuration, and (d) displays the light pattern for a magnetic tripolar configuration. Here "monopolar configuration" means that only one pole is affecting the light pattern. The light source is positioned at the top in figures (b), (c), and (d)

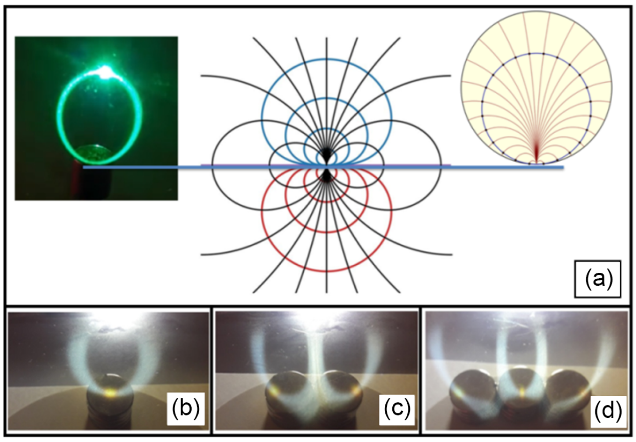

have a magnet on a thin ferrofluid film, with a set of white LEDs arranged circularly around the magnetic bar forming the light pattern of a dipole. A parallel can be drawn between compass needles and ice crystals aligning with electric fields in clouds. The fundamental analogies lie in the presence of interacting dipoles within a field, where the system exhibits various states of order and disorder, as shown in Table 1.

Figure 10

(a) Light pattern in a film of ferrofluid in the presence of a magnetic field. (b) Zooming the light pattern, we can see the micrometric needles. (c) A table of a square lattice of small compass in the presence of a magnetic coil. (d) Light pattern for a magnetic dipole in the ferrofluid with circular array of LEDs. Considering the light source and the magnetic field, the light pattern is always perpendicular to the field, this is related to the fact that the particles from small needles that align with the applied field. This leads us to consider a model of compass needles in a square lattice

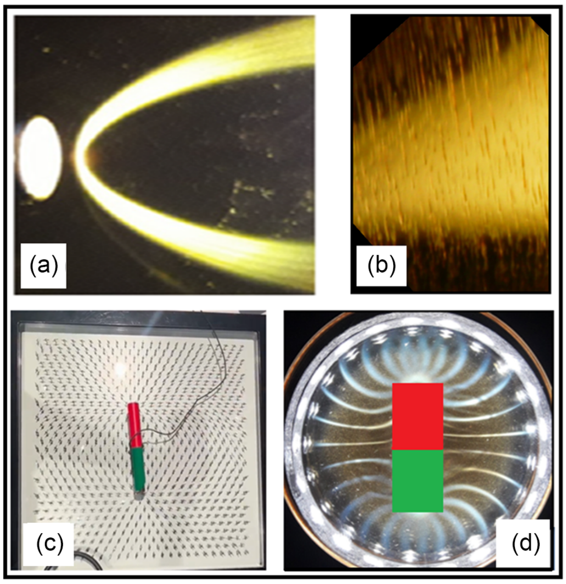

Figure 11 highlights the interaction between ferrofluid microneedles under a changing magnetic field. The two upper images showcase the needles in the green ellipses region attracting each other.

To close this section, we will exemplify the optical case of whip-like motion in ferrofluid. The whip-like motion can be observed in ferrofluids subjected to a dipole field when the field's orientation changes slightly, as shown in Figure 12. The image sequence depicts this process in Figure 12(a) for the case of the initial horocycle pattern, in which a horocycle forms due to a stronger magnetic pole positioned near the ferrofluid plate. After that we have in Figure 12(b) the disruption of the Horocycle, because as the field changes slightly, this change disrupts the initial horocycle pattern. In Figures 12(c) and (d), we have a transition to open curve, because with both poles affecting the ferrofluid equally, the pattern transforms into an open curve shape. In Figure 12(e), there is a diagram of the whip-like motion. This diagram illustrates the sequence of light patterns observed during the process. The key to the whip-like motion lies in the green curve marked "2" in Figure 12(e). This unstable pattern represents a sudden transition, similar to shifting from a single potential well (area of attraction) to a double-well potential, where the ferrofluid experiences two competing forces. This abrupt change is what causes the whiplash movement. Viewers can observe this effect in a video titled 'Whip-like motion in light pattern produced by ferrofluid thin film' which is available on YouTube. A link to this video is provided in the Data Availability Statement.

Table 1
Comparison between magnetic needles and ice crystals

Element	Magnetic needles	Ice crystal
External Field	From the magnet	Electric field in clouds
Dipole	Magnetic moment	Electric moment
Ordered state	Magnetic needles aligned with the magnet's magnetic field.	Ice crystals aligned with the electric field. (Ferroelectric state)
Disordered state	Randomly oriented magnetic needles	Randomly oriented ice crystals. (Paraelectric state)

Figure 11
The dipolar magnetic needles are analogous to the case of microneedles formation in a film of diluted ferrofluid solution in the presence of a magnetic field as we can see in (a). By changing the orientation of the magnetic field, the microneedles change their orientation in (b). (c) We can see a smoother variation in the orientation of the magnetic field shown by the arrows next to the images of the microneedles, for seven different magnetic fields

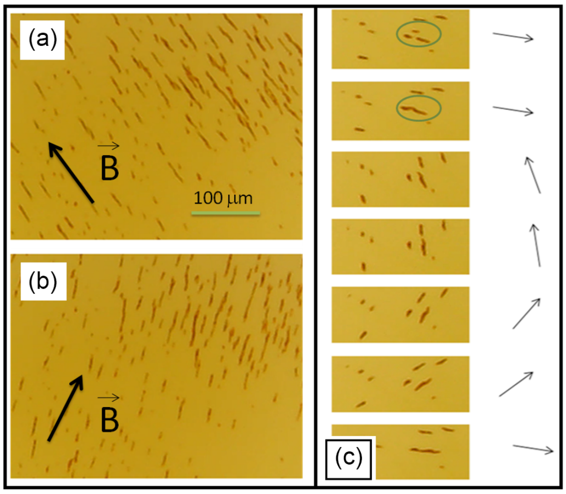

5. Ising Model for a Cloud

The main goal of this section is to propose a simplified model to explain how a specific set of crystals aligns with an electric field. We will use the two-dimensional Ising model for this purpose. The 2D Ising model can be adapted to simulate a system with fixed "compass needles" arranged in a square lattice [26, 27]. In the Ising model, spins are discrete variables representing magnetic moments. Imagine these spins as compass needles pointing in different directions. We can arrange these needles on a square lattice, allowing each needle to point in only two directions. To set up this model, we represent our system as a 2D square lattice, where each lattice site corresponds to a compass needle. We associate a spin variable with each lattice site, with each spin taking one of two values representing the needle's orientation (e.g., up or down). We then define an energy function describing the interaction between neighboring compass needles. This function can favor alignment (ferromagnetic interaction) or misalignment (antiferromagnetic interaction). Finally, we introduce a temperature parameter that influences the probability of spin flips. At higher temperatures, spins are more likely to change orientation.

The Ising model and leaping sundogs share key characteristics: both involve discrete elements (spins and ice crystals) exhibiting collective behavior. The Ising model can simplify the complex dynamics of atmospheric optics, focusing on essential features like ice crystal orientation and interaction. By parameterizing the

Figure 12
Example of whip-like motion optics in the case of ferrofluid in the presence of dipole field for small changes in the orientation of the dipole field. The sequence of images firstly in (a) the horocycle pattern which is formed by the existence of a pole more intense than the other close to the ferrofluid plate, in (b) we have a region that destroys the horocycle, leading it to a pattern of an open curve in (c) and (d) when both poles affect the ferrofluid equivalently. The diagram in (e) shows this sequence of light patterns. The green curve marked with the number 2 is an unstable pattern that represents the abrupt transition that gives the whiplash movement, as if we had a transition from a single potential to a double potential

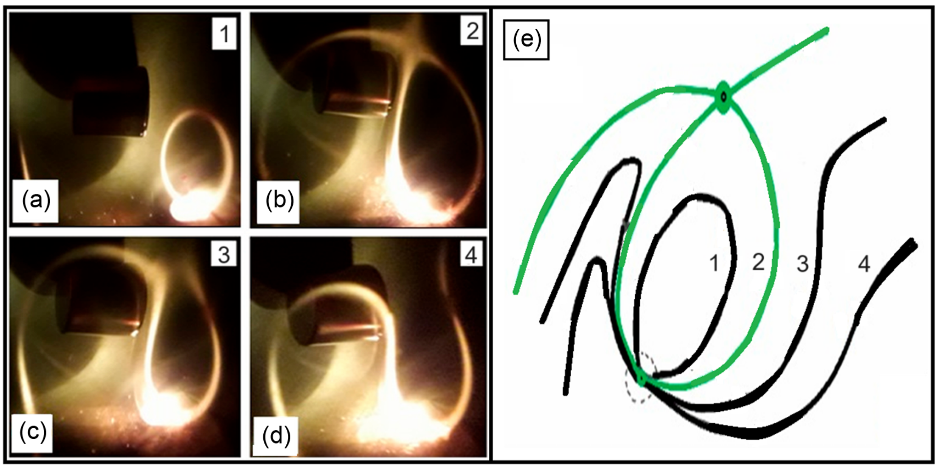

Figure 13
Plots of average energy graphs in (a) and average spin in (b) for temperature $T = 0.169$ using the Ising model, showing the evolution of spin alignment from an initial condition. The inset in (b) represents the square lattice of upward-pointing spins (−1) in its final state, which forms a white square

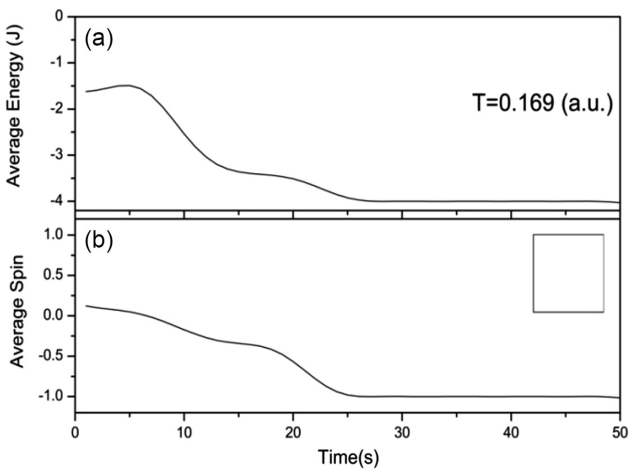

model, we can analyze the statistical properties of leaping sundogs, make predictions, and gain insights into their occurrence under different atmospheric conditions. While the Ising model offers a valuable tool, it’s important to acknowledge its limitations and the need for further research to fully comprehend the intricate mechanisms behind leaping sundogs.

This simulation is the implementation of a two-dimensional Ising model for a table with compass needles arranged in a two-dimensional lattice for different temperature values shown for “average spin” and “average energy” are shown in Figures 13–15. The model employs the Metropolis Monte Carlo algorithm to update the spin lattice. The spin lattice comprises spins with

Figure 14
Plots of average energy in (a), and average spin in (b) for the critical temperature $T_c = 2.269$ using the Ising model. The inset in (b) represents the square lattice of spins at the critical temperature T_c, showing a pattern of clusters of −1 spins (white region) and +1 spins (black region). Typically, T_c separates ordered (ferromagnetic) and disordered (paramagnetic) phases

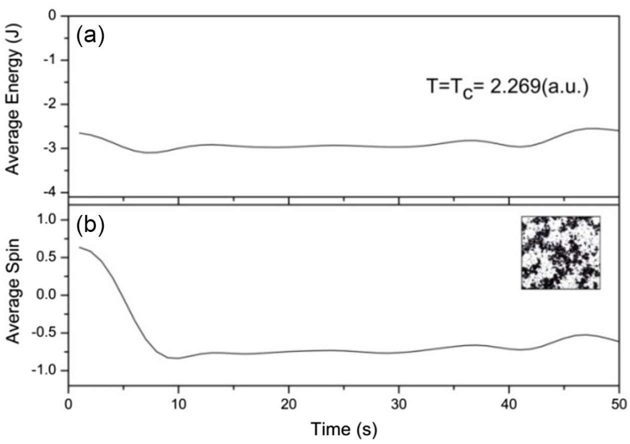

Figure 15
(a) and (b) depict the Ising model’s behavior at a temperature (T) of 5.669. The plot in (a) shows the average energy, while (b) displays the average spin. The inset in (b) visualizes a randomly oriented square lattice of spins. This scenario represents a temperature exceeding the critical temperature (T_c). At temperatures above T_c, thermal fluctuations become significant. Spins flip more often, resulting in a paramagnetic phase. In this phase, the spins are predominantly random and lack a clear preference for alignment

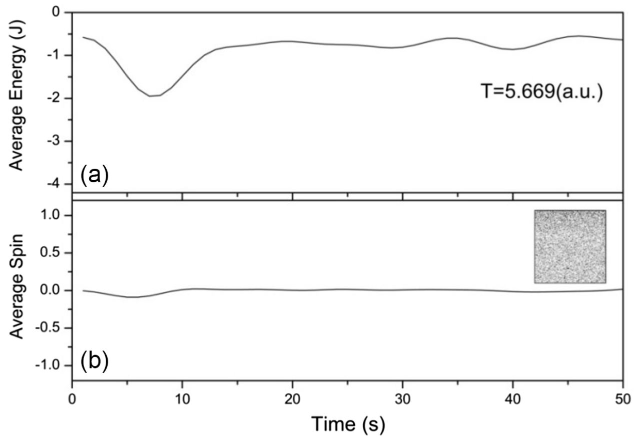

values of either +1 (black) or −1 (white). The spins can be initially configured as all up, all down, or randomly up and down at any point during the computation.

The Metropolis algorithm iterates through all cells of the lattice, executing the following steps. First, for each cell, the energy configuration is computed for the current spin and with the spin flipped. Second, if the energy difference $\Delta(Energy)$ is less than zero or if the value $e^{-\beta\Delta(Energy)}$ is greater than a random number, the spin of the cell is flipped. This exponential tells you how probable it is for a spin to flip based on the energy change caused by the flip and the overall system temperature (represented by β). When the temperature is set well above the critical value, the spin arrangement tends towards a nearly random state, independent of the initial configuration. Consequently, above the critical temperature, a single thermodynamic stage with zero magnetization emerges.

Setting the temperature below the critical value results in the system converging to either an up or down spin state, depending on its initial state. Two thermodynamic states exist, and the system remains in one based on initialization. Starting below the critical temperature with a warm (random) spin initialization leads to initial instability. Eventually, one state becomes prevalent with equal probability, as shown in Figure 13.

Drawing an analogy from magnetism to electricity, let’s explore how ice crystals in jumping sundogs might orient themselves. Similar to magnetic materials, ice crystals could exhibit a critical temperature of Figure 14. Below this temperature, they might align in a specific direction (ferroelectric behavior), while above it, they would orient more randomly (paraelectric behavior), as shown in Figure 15. The presence of an electric field created by the charges within the cloud could disrupt the orientation of columnar or needle-shaped ice crystals above the cloud, as was expressed in Equations (4) and (5). These crystals, due to aerodynamic reasons, tend to align with their long axis parallel to the ground. The electric field generated by nearby charges could potentially influence the crystals’ behavior in both ferroelectric (aligned) and paraelectric (random) states.

Figure 16
We can observe a connection between hysteresis and a supercritical pitchfork bifurcation. In diagram shown in (a), the system evolves towards a single stable fixed point when the control parameter h is less than zero (h < 0). As we increase the control parameter h shown in diagram (b), a saddle-node bifurcation occurs. The complete hysteresis cycle depends on the history of the initial conditions, as shown in (c), along with the Barkhausen jump with the two stable branches (1) and (2). In (d), it depicts the pitchfork bifurcation for each branch of the hysteresis cycle. In (e), the average spin of the ice crystals represents the memory effect for each stable branch (1) and (2)

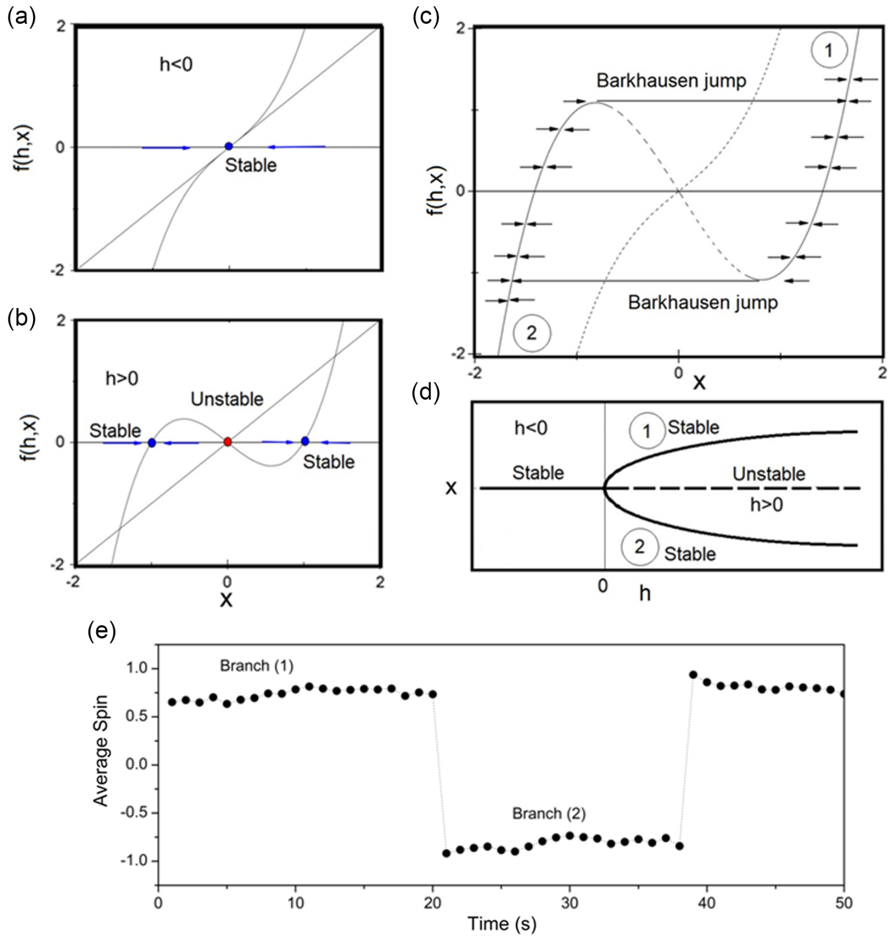

Furthermore, the movement of electric charges within the cloud, particularly at the base of the jumping sundog plume, might be responsible for the phenomenon's characteristic motion. The interaction of the electric field with the ice crystals, possibly including their multipolar moments, could be the driving force behind the observed whip-like or flaming movements. These movements of jumping sundogs might be linked to two factors: (a) interactions between air currents and electrical charges within the cloud and (b) reorientations of these charges due to low-intensity electrical discharges, similar to faint lightning strikes occurring within the cloud.

If these two temperature-dependent phases (possibly ferroelectric and paraelectric) exist for the ice crystals, the jumping sundog's behavior might exhibit hysteresis in the ferroelectric phase. This means its orientation for a given electric field could depend on its previous state. In simpler terms, the jumping sundog might 'remember' its past orientation in the ferroelectric phase, unlike the paraelectric phase where it would always return to the same position for the same electric field.

Until this point, our current understanding suggests that an external electric field might be influencing the dramatic reorientation of ice crystals within jumping sundogs. However, an intriguing alternative theory emerges from the realm of critical phenomena. This theory proposes that the ice crystals themselves, upon reaching a critical temperature within the cloud, could undergo a phase transition without the necessity of an external electric field.

Let's consider critical opalescence as an example to illustrate this concept further. This phenomenon occurs near the critical point of a material, a specific temperature and pressure combination where two distinct phases (like liquid and gas) become indistinguishable. As light travels through this material, its direction can be scattered by the density fluctuations within. This kind of bistable system is related with pitchfork bifurcation [28].

The average energy and spin of the system depend on temperature. At lower temperatures, energy levels are lower. The average spin can undergo transitions with varying stability, as shown in Figure 16. Critical phenomena involve drastic changes in properties near a critical point. For jumping sundogs, this point could be a specific temperature. At this temperature, even small fluctuations can trigger significant reorientations of ice crystals, resulting in the observed movements. This suggests that jumping sundogs are not just a response to an external field but a manifestation of a fundamental property of ice crystals at their critical temperature or other parameters.

Based on this average spin, we can say that ice crystals lack positional order. This means the crystals aren't arranged in a regular lattice. However, they do exhibit some degree of orientational order, similar to the "director" in liquid crystal terminology, a unit vector which defines the average orientation of the elongated, hexagonal columns within the cloud. This reminds us that we can find other systems where crystallization or nucleation of ice crystals or drops, and organization phenomena occur in the most diverse environments [29–35]. The whipping behavior of jumping sundogs can be interpreted as Barkhausen jumps in the ferroelectric state [36, 37]. The paraelectric state can be interpreted as the ice crystals in the state that creates the regular 22-degree halo and the static sundogs, which do not undergo abrupt changes. This could explain the overlapping of leaping sundogs concomitantly with regular halos and static sundogs, based on phase transitions related to bifurcations in some kinds of matter [38–42]. This implies that by understanding the factors influencing jumping sundogs, such as ice crystal formation, atmospheric conditions, and light interactions, we can potentially develop models or systems that can predict their appearance, similar to how people intend to track auroras [43].

6. Conclusions

Inspired by social media videos, we explored the phenomenon of jumping sundogs using ferrofluids and ice crystal dynamics. We propose that ice crystals, behaving like tiny dipolar needles, might undergo phase transitions influenced by temperature and electric fields within clouds.

Below a critical temperature, these crystals align in a specific direction. However, above this temperature, they become randomly oriented. Electric fields from cloud charges can disrupt this order, leading to the rapid, whip-like motions observed in jumping sundogs. The movement of charges within the cloud, potentially involving faint lightning-like discharges, could also contribute to these shifts.

This temperature-dependent behavior suggests a memory effect, where the crystals' orientation depends on their past state. Jumping sundogs might be a type of critical phenomenon, where small changes in environmental conditions can lead to dramatic shifts in crystal alignment. The rarity of jumping sundogs could be attributed to the specific conditions required: a critical temperature range and the presence of disruptive electric fields.

By combining ferrofluid experiments and statistical mechanics, we offer a novel and comprehensive explanation for jumping sundogs. This research opens new avenues for understanding the complex interplay between ice crystals, electric fields, and atmospheric phenomena.

Ethical Statement

This study does not contain any studies with human or animal subjects performed by any of the authors.

Conflicts of Interest

The authors declare that they have no conflicts of interest to this work.

Data Availability Statement

List of jumping sundogs videos at https://www.researchgate.net/publication/381039244_Jumping_Sundogs_List_of_Videos. Data are available from the corresponding author upon reasonable request.

Author Contribution Statement

Alberto Tufaile: Conceptualization, Methodology, Software, Validation, Formal analysis, Investigation, Resources, Data curation, Writing – original draft, Writing – review & editing, Visualization, Supervision, Project administration. **Adriana Pedrosa Biscaia Tufaile:** Conceptualization, Methodology, Validation, Formal analysis, Resources, Data curation, Writing – review & editing, Visualization, Project administration.

References

[1] Tufaile, A., Snyder, M., Vanderelli, T. A., & Tufaile, A. P. B. (2020). Jumping sundogs, cat's eye and ferrofluids. *Condensed Matter*, *5*(3), 45. https://doi.org/10.3390/condmat5030045

[2] Libbrecht, K. G. (2017). Physical dynamics of ice crystal growth. *Annual Review of Materials Research*, *47*, 271–295. https://doi.org/10.1146/annurev-matsci-070616-124135

[3] Guo, T., Zheng, X., & Palffy-Muhoray, P. (2021). The Freedericksz transition in a spatially varying magnetic field. *Crystals*, *11*(5), 541. https://doi.org/10.3390/cryst11050541

[4] Cook, G., Reshetnyak, V. Y., Ziolo, R. F., Basun, S. A., Banerjee, P. P., & Evans, D. R. (2010). Asymmetric Freedericksz transitions from symmetric liquid crystal cells doped with harvested ferroelectric nanoparticles. *Optics Express*, *18*(16), 17339–17345. https://doi.org/10.1364/OE.18.017339

[5] Petrescu, E., Cirtoaje, C., & Stan, C. (2017). Dynamic behavior of a nematic liquid crystal mixed with $CoFe_2O_4$ ferromagnetic nanoparticles in a magnetic field. *Beilstein Journal of Nanotechnology*, *8*, 2467–2473. https://doi.org/10.3762/bjnano.8.246

[6] Binney, J. J., Dowrick, N. J., Fisher, A. J., & Newman, M. E. J. (1992). *The theory of critical phenomena: An introduction to the renormalization group*. UK: Oxford University Press. https://doi.org/10.1093/oso/9780198513940.001.0001

[7] Lipowski, A. (2022). Ising model: Recent developments and exotic applications. *Entropy*, *24*(12), 1834. https://doi.org/10.3390/e24121834

[8] Paszkiewicz, A. (2021). Modeling and analysis of anomalies in the network infrastructure based on the Potts model. *Entropy*, *23*(8), 949. https://doi.org/10.3390/e23080949

[9] Valle, M. A., Lavín, J. F., & Magner, N. S. (2021). Equity market description under high and low volatility regimes using maximum entropy pairwise distribution. *Entropy*, *23*(10), 1307. https://doi.org/10.3390/e23101307

[10] Dutta, S., & Gellman, A. J. (2022). 2D Ising model for enantiomer adsorption on achiral surfaces: L- and D-aspartic acid on Cu(111). *Entropy*, *24*(4), 565. https://doi.org/10.3390/e24040565

[11] Li, D., Saito, M., & Yang, P. (2023). Time-dependent systematic biases in inferring ice cloud properties from geostationary satellite observations. *Remote Sensing*, *15*(3), 855. https://doi.org/10.3390/rs15030855

[12] Jiang, Y., & Yi, B. (2023). An assessment of the influences of clouds on the solar photovoltaic potential over China. *Remote Sensing*, *15*(1), 258. https://doi.org/10.3390/rs15010258

[13] Jang, S., Kim, J., McFarquhar, G. M., Park, S., Han, S., Lee, S. S., . . . , & Um, J. (2022). The impacts of single-scattering and microphysical properties of ice particles smaller than 100 µm on the bulk radiative properties of tropical cirrus. *Remote Sensing*, *14*(13), 3002. https://doi.org/10.3390/rs14133002

[14] Wang, Y., Yang, P., King, M. D., & Baum, B. A. (2021). Optical property model for cirrus clouds based on airborne multi-angle polarization observations. *Remote Sensing*, *13*(14), 2754. https://doi.org/10.3390/rs13142754

[15] Baran, A. J. (2009). A review of the light scattering properties of cirrus. *Journal of Quantitative Spectroscopy and Radiative Transfer*, *110*(14–16), 1239–1260. https://doi.org/10.1016/j.jqsrt.2009.02.026
[16] Sun, L.-H., Bi, L., & Yi, B. (2021). The use of superspheroids as surrogates for modeling electromagnetic wave scattering by ice crystals. *Remote Sensing*, *13*(9), 1733. https://doi.org/10.3390/rs13091733
[17] Liu, L., Weng, C., Li, S., Husi, L., Hu, S., & Dong, P. (2021). Passive remote sensing of ice cloud properties at terahertz wavelengths based on genetic algorithm. *Remote Sensing*, *13*(4), 735. https://doi.org/10.3390/rs13040735
[18] Wirowski, A. (2014). The dynamic behaviour of the electrically charged cloud of the ice crystals. *Applied Mathematics and Physics*, *2*(1), 19–26.
[19] Tufaile, A., Snyder, M., & Tufaile, A. P. B. (2021). Horocycles of light in a ferrocell. *Condensed Matter*, *6*(3), 30. https://doi.org/10.3390/condmat6030030
[20] Naumov, I. I., Bellaiche, L., & Fu, H. (2004). Unusual phase transitions in ferroelectric nanodisks and nanorods. *Nature*, *432*(7018), 737–740. https://doi.org/10.1038/nature03107
[21] Lines, M. E., & Glass, A. M. (2001). *Principles and applications of ferroelectrics and related materials*. UK: Oxford University Press. https://doi.org/10.1093/acprof:oso/9780198507789.001.0001
[22] Tufaile, A., Vanderelli, T. A., & Tufaile, A. P. B. (2018). Chaotic dynamics of ice crystals scattering sun light. *Chaotic Modeling and Simulation*, *2*, 159–171.
[23] Tufaile, A., & Tufaile, A. P. B. (2024). Investigating isogyres in ferrofluids and horocycles from parlaseric circle in a ferrocell. *Journal of Optics and Photonics Research*, *1*(4), 170–183. https://doi.org/10.47852/bonviewJOPR42022329
[24] Vonnegut, B. (1965). Orientation of ice crystals in the electric field of a thunderstorm. *Weather*, *20*(10), 310–312. https://doi.org/10.1002/j.1477-8696.1965.tb02740.x
[25] Graves, M. E., Gall, J. C., & Vonnegut, B. (1971). Meteorological phenomenon called crown flash. *Nature*, *231*(5300), 258. https://doi.org/10.1038/231258a0
[26] Olive, E., & Molho, P. (1998). Thermodynamic study of a lattice of compass needles in dipolar interaction. *Physical Review B*, *58*(14), 9238–9247. https://doi.org/10.1103/PhysRevB.58.9238.
[27] Velo, M. F., Cecchi, B. M., Béron, F., & Pirota, K. R. (2020). Multipolar effects in the hysteresis behavior of 2D arrays of compass needles: Experiments and simulations. *Physics Open*, *5*, 100041. https://doi.org/10.1016/j.physo.2020.100041
[28] Bertotti, G. (1998). *Hysteresis in magnetism: For physicists, materials scientists, and engineers*. USA: Academic Press. https://doi.org/10.1016/B978-0-12-093270-2.X5048-X
[29] Yin, K., Ji, K., Littles, L. S., Trivedi, R., Karma, A., & Wegst, U. G. K. (2023). Hierarchical structure formation by crystal growth-front instabilities during ice templating. *Proceedings of the National Academy of Sciences*, *120*(23), e2210242120. https://doi.org/10.1073/pnas.2210242120
[30] Freitas, R., & Reed, E. J. (2020). Uncovering the effects of interface-induced ordering of liquid on crystal growth using machine learning. *Nature Communications*, *11*(1), 3260. https://doi.org/10.1038/s41467-020-16892-4
[31] Loftus, K., & Wordsworth, R. D. (2021). The physics of falling raindrops in diverse planetary atmospheres. *Journal of Geophysical Research: Planets*, *126*(4), e2020JE006653. https://doi.org/10.1029/2020JE006653
[32] Zueter, A. F., Xu, M., Alzoubi, M. A., & Sasmito, A. P. (2021). Development of conjugate reduced-order models for selective artificial ground freezing: Thermal and computational analysis. *Applied Thermal Engineering*, *190*, 116782. https://doi.org/10.1016/j.applthermaleng.2021.116782
[33] Mochizuki, K., Murata, K., & Zhang, X. (2023). Microscopic ordering of supercooled water on the ice basal face. *Communications Materials*, *4*(1), 33. https://doi.org/10.1038/s43246-023-00359-2
[34] Llombart, P., Noya, E. G., & MacDowell, L. G. (2020). Surface phase transitions and crystal habits of ice in the atmosphere. *Science Advances*, *6*(21), eaay9322. https://doi.org/10.1126/sciadv.aay9322
[35] Roisman, I. V., & Tropeano, C. (2021). Wetting and icing of surfaces. *Current Opinion in Colloid & Interface Science*, *53*, 101400. https://doi.org/10.1016/j.cocis.2020.101400
[36] Fagan, P., Zhang, S., Sebald, G., Uchimoto, T., & Ducharne, B. (2023). Barkhausen noise hysteresis cycle: Theoretical and experimental understanding. *Journal of Magnetism and Magnetic Materials*, *578*, 170810. https://doi.org/10.1016/j.jmmm.2023.170810
[37] Maciusowicz, M., & Psuj, G. (2019). Use of time-dependent multispectral representation of magnetic Barkhausen noise signals for the needs of non-destructive evaluation of steel materials. *Sensors*, *19*(6), 1443. https://doi.org/10.3390/s19061443
[38] Korenjak, Z., & Humar, M. (2024). Smectic and soap bubble optofluidic lasers. *Physical Review X*, *14*(1), 011002. https://doi.org/10.1103/PhysRevX.14.011002
[39] Alam, S., Najma, B., Singh, A., Laprade, J., Gajeshwar, G., Yevick, H. G., . . . , & Duclos, G. (2024). Active Fréedericksz transition in active nematic droplets. *Physical Review X*, *14*(4), 041002. https://doi.org/10.1103/PhysRevX.14.041002
[40] Bowick, M. J., Fakhri, N., Marchetti, M. C., & Ramaswamy, S. (2022). Symmetry, thermodynamics, and topology in active matter. *Physical Review X*, *12*(1), 010501. https://doi.org/10.1103/PhysRevX.12.010501
[41] Chatterjee, R., Rana, N., Simha, R. A., Perlekar, P., & Ramaswamy, S. (2021). Inertia drives a flocking phase transition in viscous active fluids. *Physical Review X*, *11*(3), 031063. https://doi.org/10.1103/PhysRevX.11.031063
[42] Zhang, J., Yang, J., Zhu, Z., Shen, G., & Sanjuán, M. A. F. (2020). Effects of different fast periodic excitations on the pitchfork bifurcation and vibrational resonance. *International Journal of Bifurcation and Chaos*, *30*(06), 2050092. https://doi.org/10.1142/S0218127420500923
[43] Ivarsen, M. F., St-Maurice, J.-P., Hussey, G. C., Huyghebaert, D. R., & Gillies, M. D. (2024). Point-cloud clustering and tracking algorithm for radar interferometry. *Physical Review E*, *110*(4), 045207. https://doi.org/10.1103/PhysRevE.110.045207

How to Cite: Tufaile, A., & Tufaile, A. P. B. (2026). Optics of Jumping Sundogs. *Journal of Optics and Photonics Research*, *3*(1), 19–29. https://doi.org/10.47852/bonviewJOPR52024594